Solid Freeform Fabrication 2023: Proceedings of the 34th Annual International Solid Freeform Fabrication Symposium – An Additive Manufacturing Conference
Reviewed Paper

In-situ Reinforcement Processing for Laser Powder Bed Fused Ti64 Parts

A. Ganesh-Ram*, A.A. Tanrikulu^†, O. Valdez Loya*, P. Davidson*, A. Ameri*†

*Mechanical & Aerospace Engineering, University of Texas at Arlington, Arlington, TX.
†Materials Science and Engineering, University of Texas at Arlington, Arlington, TX.
^Turkish Aerospace Industries, Ankara, Turkey.

Abstract

The objective of this study was to investigate how the microstructure and mechanical properties of Ti-6Al-4V samples, fabricated using laser powder bed fusion (L-PBF), change when a predefined local double melting strategy is employed within each layer of the manufacturing process. The analysis primarily focused on evaluating microstructural aspects, defects, and grain size, along with the mechanical properties, specifically the Vickers hardness at various positions within the samples. The findings indicated that the integration of the predefined locally double melting scan in each layer had a significant influence on the microstructure, resulting in variations in grain size across different locations, as well as hardness values with variations of up to 10% across different areas. Moreover, these discoveries underscore the potential of employing the predefined locally double melting strategy in each layer to create fabricated components with distinctive behaviors, like composites, which could find applications in the aerospace industry.

Keywords: Laser powder bed fusion, In-situ strengthening, Ti6Al4V.

1. Introduction

Ti6Al4V(Ti64) have positioned itself as the most advantageous Titanium alloy in the recent decades due to its demand in the aerospace and the biomedical industries [1-2]. The combination of both α and β phases in the alloy combination makes it more versatile for the varied mechanical properties that can be given rise with a control over the thermal processing strategies [3]. The laser processability of the alloys had paved breakthrough pathways to fabricate complex near net shape parts using Laser Powder Bed Fusion (LPBF). Numerous reviews have been made available discussing the use of the alloy in Additive Manufacturing(AM) [4–6].

LPBF has long been used as a successful additive manufacturing process for metals that can bring about micro-sized features at the expense of the limiting laser spot size. A wide variety of alloys are being developed for the process making it a promising AM technique adoption. Therefore, the process have also been developed further to make it time saving for shorted lead time using multiple lasers or area wise processing with the only limitation being the laser spot size [7-8]. On the other hand, the process contributes lower amount of carbon dioxide to the atmosphere than conventional manufacturing process for Titanium alloys [9]. This makes it more advantageous and low carbon footprint process unlike others.

Post heat treatment is a commonly used after fabrication stage for Ti64 to achieve the desired microstructural phases of the LPBFed part [10]. But it is usually a time-consuming process used right after the fabrication raising the lead time for a finished and processed end part [11]. The conventional heat treatment processes involve raising the temperature of the part and maintaining it at certain time cycles for the desired microstructural phases based on the cooling rate induced. This requires additional cost and time before the final part arrives in hand. The process flow of the LPBF itself paves way for thermal processing by tweaking the laser parameters during fabrication. Since the laser can be controlled over the coordinates of the build plater to bring about the necessary thermal behavior at different regions, the extent of its relationship with strengthening a part layer by layer have been ideated here. An in-situ microstructural strengthening technique that can bring about desired phases of Titanium drawing parallels with a steel bar strengthening a concrete pillar which could result in a better mechanical property would be a great time and cost saving technique for LPBF. Here, such processing where a strengthening matrix like laser processing on the Ti64 parts has been studied. The results drawn from the study proved that a fabricated part can be strengthened with a refined material in a localized region. This brings about a microstructural based location wise control forming a supporting matrix for the entire part similar to a fiber reinforced composite[12].

2. Materials and Methods

2.1 Powder and Fabrication Process

The powder used for the fabrication of parts in this study, is Grade 5 Ti64 provided by EOS GmbH. Particle size distribution of the powder had been ensured using a sieve size of 80 µm. Based on a prior powder particle distribution analysis using SEM, the particle size ranged between 35 µm and 45 µm. A mix of fresh and reused powder after sieving had been added to dispense for fabrication of the parts using EOS M290. The powder composition as mentioned by the provider is added in table 1.

Table 1. Composition of elements in the Ti-6Al-4V powder material purchased from EOS.

Element	Ti	Al	V	O	N	C	H	Fe
Concentration	Balance	5.5 – 6.75 wt.%	3.5 – 4.5 wt.%	< 2000 ppm	< 500 ppm	< 800 ppm	< 150 ppm	< 3000 ppm

2.2 Parts and Fabrication Parameters

In order to study the effect of double exposing on the mechanical property of the fabricated samples, 2 different variations have been studied. One is named DEB which has wider double exposed regions and other one is named as DES which has narrower double exposed regions. The dimension of the coupons used in this study have been shown in the figure. The light grey region with dashed arrows is first exposed with laser parameter set A and the dark grey regions with solid

black arrows are exposed a second time in the coupons with parameter set B. So, the darker regions are exposed twice.

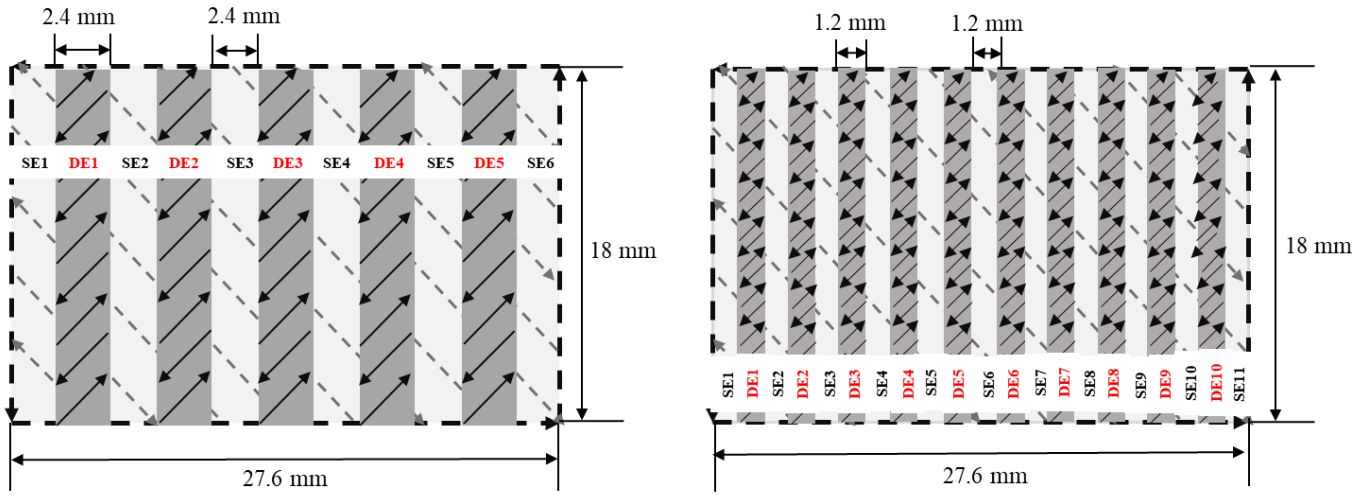

Fig. 1: Coupon Dimensions – DEB(Left); DES(Right)

The parameter set A is suggested by EOS for the Grade 5 Ti6Al4V powder supplied by them. The set B has been used arbitrarily as 85% reduction in the laser power keeping everything else as is. Set A was processed with a contour using EOS suggested laser parameters for the contour processing and Set B was processed without any contour. So, layer by layer, the sample had been laser processed once with set A and the darker region a second time with set B. Each of the alternating regions have been named as SE for single exposed and DE for double exposed region with the number indicating its position in the sample.

Table 2: Laser Fabrication Parameter sets used

Parameter Set	Laser Power (W)	Scan Speed (mm/s)	Hatch Distance (mm)	Laser Energy (J/mm^3)
A	280	1300	0.12	44.87
B	238	1300	0.12	38.14

2.5 Microstructure, Phase and Mechanical Property Analysis

The region perpendicular to the building direction away from the build plate of the fabricated coupons have been polished until 0.04 µm colloidal silica solution. The samples were then optical micro graphed at various DE and SE regions to study the porosity of the samples at those regions. Image J has been used to measure the 2D surface porosity in different regions of the sample. The samples have also been studied under Scanning Electron Microscope for phases of the material. The captured images at 800 and 900 magnification level have been used to calculate the lath size distributions using Image J.

One of the double and single exposed regions from the DEB samples have been cut out from the center to measure the X-ray diffractions due to grain structures formed only due to double exposing and single exposing. The XRD analysis have been performed with Bruker D8 system on both those cut out regions to analyze the effect of the varied laser processing at the lattice level.

Vickers Microhardness analysis was used to characterize the mechanical hardness property of the regions in the coupons. At least 6 indentations were made in each alternative single and double exposed regions of the same sample to capture the hardness variation across the sample perpendicular to the build direction.

3. Results and Discussion

The double exposed regions of the sample can be clearly distinguished from the single exposed regions right out of fabrication by visual inspection. The surface depicted a similarity of that as a carbon reinforced composite where the alternate fiber weave can be visually identified. So, a composite looking like parts has been the resulting parts out of this processing techniques with the mechanical property results supporting it.

3.1 Hardness Variation

The micro-hardness indentations made across the specimens reveal that hardness property of a region varied depending on the laser processing conditions in or around the region. It has been observed in the DEB specimen that the hardness of the coupons had a zigzag trend across the coupons with crests at the double exposed regions and the troughs at the single exposed regions. Whereas the DES specimen showed a collective concentration of the hardness property over a set of alternative single and double exposed regions. The trend observed in the DEB specimen, clearly shows that either microstructural phase strengthening, or a defect density reduction seem to be resulting in an improvement of micro-hardness values in the double exposed regions. The hardness of the surface perpendicular to the building direction at the region away from the building plate at the sample processed with only set A for reference have also been indicated with a red box marker in fig 2.

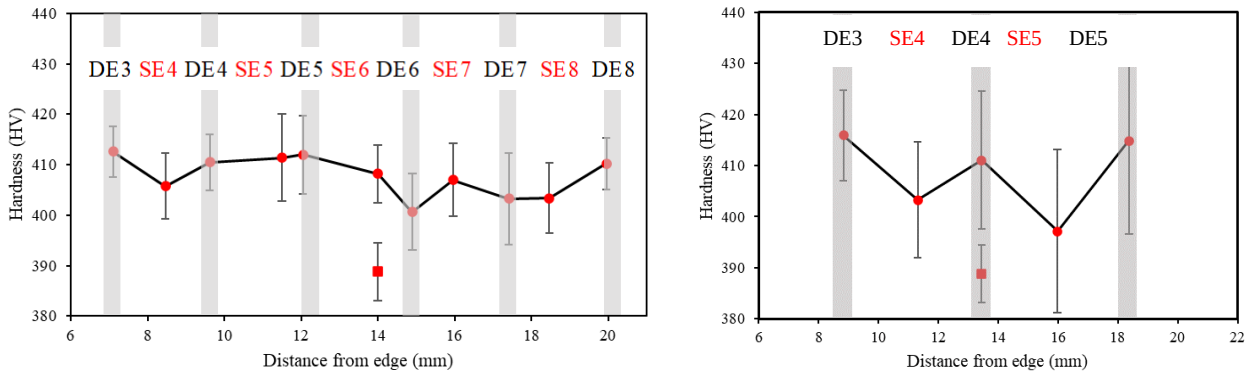

Fig 2: Micro-hardness results for DES (left) and DEB (right)

The micro-hardness indentations made in the coupons reveal that there is a distinguishable variation of hardness values depending on the width of the double exposed regions. The coupons with wider double exposed regions (DEB) seem to have better control over the mechanical hardness of the regions. The narrower double exposed strips give rise to higher heat transfer to the adjacent regions thus contributing to changes in hardness collectively over a set of strips. The width of the double exposed regions was found to be the limiting factor for controlling the hardness. This could be attributed to the defect density or the resulting grain structure as a result varied cooling rates in different regions.

3.2. Hardness and Porosity

As mentioned previously, in order to closely study the contributing factor towards increasing hardness the porosity of the regions have been mapped. 2D surface porosity of some of the regions focused to the middle portion of both the DEB and DES samples have been attached in figure. It is observed that as the region's porosity increased, the hardness of those regions also increased. It can be observed that the mechanical hardness property was found to be directly proportional to the defect density in the region. Whereas *Javidrad et al.* concluded that the defect density affects the hardness with direct proportionality [13]. so clearly microstructural phases seem to have a huge impact in the hardness improvement for those regions.

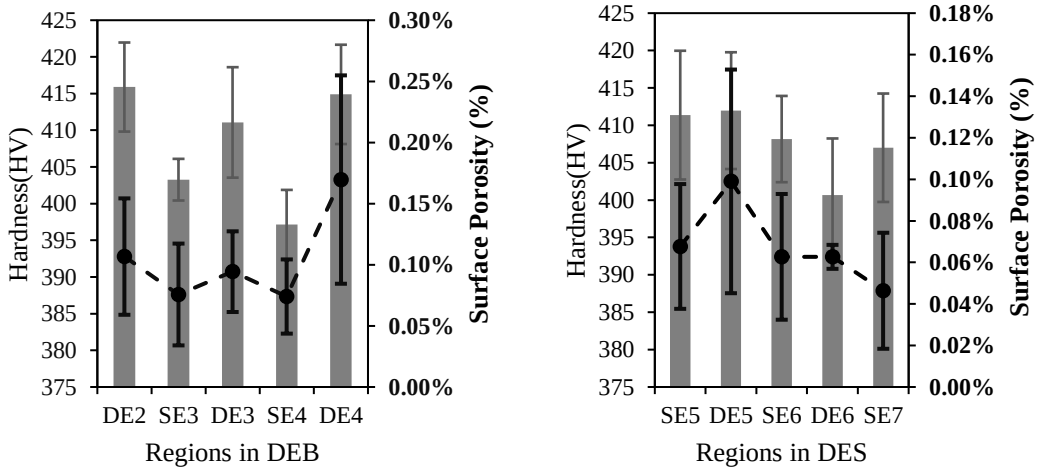

Figure 3 : Hardness and Porosity over the regions of DEB (Left) and DES Sample

3.3. α Lath sizes and Microstructure

To study the microstructural phases, the scanning electron microscope images captured from the DE and SE regions of the DEB sample have been studied for the Lath thickness. It has been found that DE regions have finer α lath sizes compared to SE regions. It should also be noted that the double exposed regions had a dark microstructural feature which was not identified in SE region as commonly as in the DE region. The feature has been identified with a red border on the images in Figure 4 (a) and (b). It is believed that such microstructural features lead to finer laths in those regions.

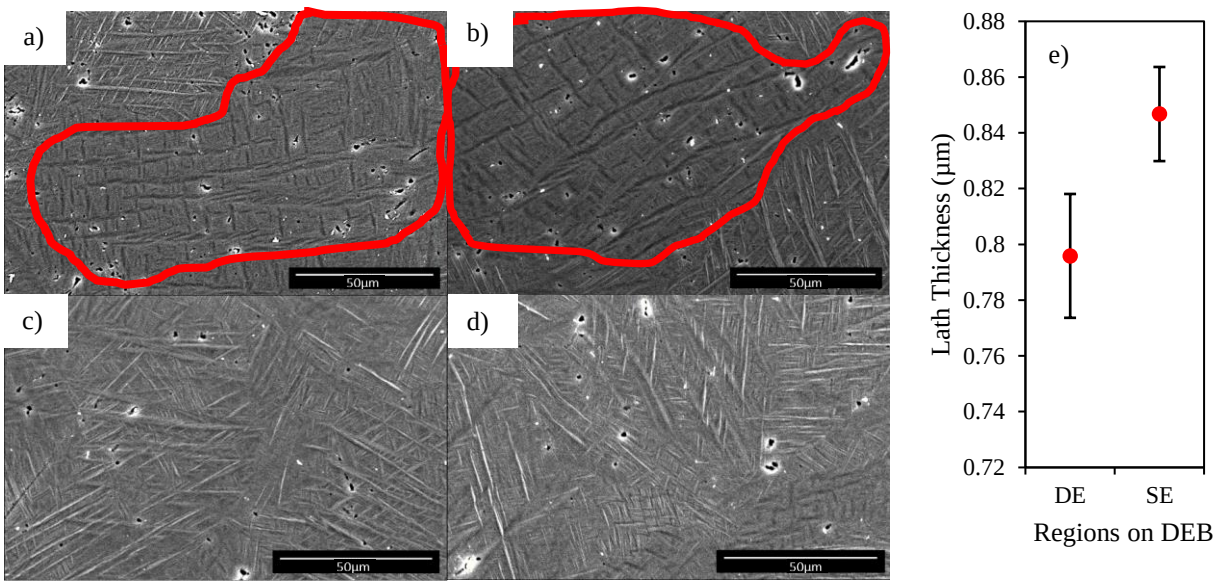

Figure 4: a) and b) – SEM image from DE3 region of DEB sample; c) and d) – SEM image from SE4 region of DEB sample; e) Lath Thickness of DE and SE regions

3.4. Phase analysis

X-ray diffractions have been measured specifically from DE and SE regions cut out from the DEB sample to study the lattice distortions and orientations. DEB sample had been selected due to its strong effect on the resulting hardness over DE regions compared to SE regions. The peaks obtained from the analysis proved that a peak narrowing has occurred after exposing the region twice with set A and set B of laser parameters. This proves that larger crystalline sizes have occurred at the DE region compared to that in the SE region using the Scherrer equation [14]. It can be concluded from the diffraction analysis that, a lattice distortion has occurred in the DE regions because of exposing it twice.

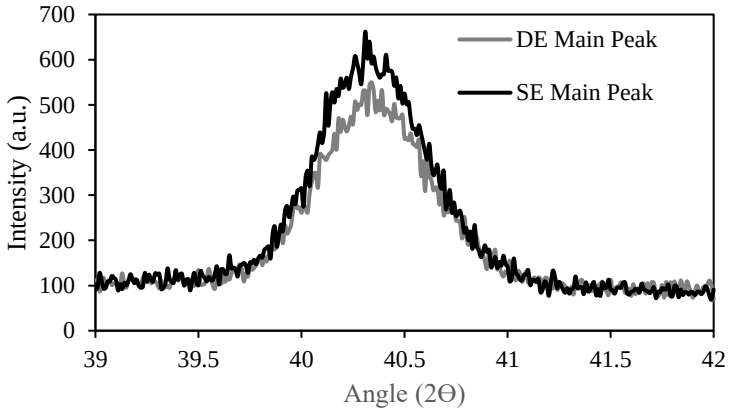

Figure 5 : XRD results from the crystalline phases of a DE and SE region in DEB

According to the Hall-Petch relationship, the crystalline size is inversely proportional to the hardness of the region [15]. The peak widening in the SE region resulted in a lower hardness value in the region as per figure 2.

4. Conclusion

The above explained in-situ laser technique during the LPBF fabrication process have been studied for it effect on the microstructural phases and the resulting mechanical properties. 2D surface porosity, lath thicknesses, lattice distortion and microhardness have been analyzed to find the resulting effect on the fabricated Ti6Al4V part due to the proposed processing technique. The highlighting conclusions from the study include:

1. The hardness of the regions scanned twice with laser was harder than the regions scanned only once
2. Porosity analysis showed that the hardness and porosity were directly related
3. Lath thickness analysis showed that double exposing resulted in finer α laths in the DE regions whereas laths were thicker in the SE regions
4. SE regions seem to have higher crystalline sizes compared to that of the DE regions based on the X-ray diffractions analyzed from the lattice structure formed

5. Acknowledgment

This work was supported by a University of Texas System STARs award.

6. References

[1] L. E. Murr *et al.*, "Microstructure and mechanical behavior of Ti–6Al–4V produced by rapid-layer manufacturing, for biomedical applications," *J. Mech. Behav. Biomed. Mater.*, vol. 2, no. 1, pp. 20–32, Jan. 2009, doi: 10.1016/j.jmbbm.2008.05.004.

[2] E. O. Ezugwu and Z. M. Wang, "Titanium alloys and their machinability—a review," *J. Mater. Process. Technol.*, vol. 68, no. 3, pp. 262–274, Aug. 1997, doi: 10.1016/S0924-0136(96)00030-1.

[3] R. Dąbrowski, "The kinetics of phase transformations during continuous cooling of the Ti6Al4V alloy from the single-phase ß range," *Arch. Metall. Mater.*, vol. Vol. 56, iss. 3, pp. 703–707, 2011.

[4] S. Liu and Y. C. Shin, "Additive manufacturing of Ti6Al4V alloy: A review," *Mater. Des.*, vol. 164, p. 107552, Feb. 2019, doi: 10.1016/j.matdes.2018.107552.

[5] T. A. Mukalay, J. A. Trimble, K. Mpofu, and R. Muvunzi, "A systematic review of process uncertainty in Ti6Al4V-selective laser melting," *CIRP J. Manuf. Sci. Technol.*, vol. 36, pp. 185–212, Jan. 2022, doi: 10.1016/j.cirpj.2021.12.005.

[6] "A short review on SLM-processed Ti6Al4V composites - M Kathiresan, M Karthikeyan, R Jose Immanuel, 2023." https://journals.sagepub.com/doi/abs/10.1177/09544089231169380 (accessed Jun. 27, 2023).

[7] C. Tenbrock, T. Kelliger, N. Praetzsch, M. Ronge, L. Jauer, and J. H. Schleifenbaum, “Effect of laser-plume interaction on part quality in multi-scanner Laser Powder Bed Fusion,” *Addit. Manuf.*, vol. 38, p. 101810, Feb. 2021, doi: 10.1016/j.addma.2020.101810.
[8] “Seurat Technologies | Area Printing | Metal Additive Manufacturing | 3D Printing,” *Seurat*. https://www.seurat.com/area-printing (accessed Jun. 27, 2023).
[9] H. Monteiro, G. Carmona-Aparicio, I. Lei, and M. Despeisse, “Energy and material efficiency strategies enabled by metal additive manufacturing – A review for the aeronautic and aerospace sectors,” *Energy Rep.*, vol. 8, pp. 298–305, Jun. 2022, doi: 10.1016/j.egyr.2022.01.035.
[10] X. Yan *et al.*, “Effect of heat treatment on the phase transformation and mechanical properties of Ti6Al4V fabricated by selective laser melting,” *J. Alloys Compd.*, vol. 764, pp. 1056–1071, Oct. 2018, doi: 10.1016/j.jallcom.2018.06.076.
[11] D. Kouprianoff and W. du Preez, “Reducing time and cost of the heat treatment post-processing of additively manufactured Ti6Al4V,” *Mater. Today Commun.*, vol. 35, p. 106186, Jun. 2023, doi: 10.1016/j.mtcomm.2023.106186.
[12] S. Erden and K. Ho, “3 - Fiber reinforced composites,” in *Fiber Technology for Fiber-Reinforced Composites*, M. Ö. Seydibeyoğlu, A. K. Mohanty, and M. Misra, Eds., in Woodhead Publishing Series in Composites Science and Engineering. Woodhead Publishing, 2017, pp. 51–79. doi: 10.1016/B978-0-08-101871-2.00003-5.
[13] H. R. Javidrad, M. Ghanbari, and F. Javidrad, “Effect of scanning pattern and volumetric energy density on the properties of selective laser melting Ti-6Al-4V specimens,” *J. Mater. Res. Technol.*, vol. 12, pp. 989–998, May 2021, doi: 10.1016/j.jmrt.2021.03.044.
[14] P. Jin *et al.*, “The relationship between the macro- and microstructure and the mechanical properties of selective-laser-melted Ti6Al4V samples under low energy inputs: Simulation and experiment,” *Opt. Laser Technol.*, vol. 148, p. 107713, Apr. 2022, doi: 10.1016/j.optlastec.2021.107713.
[15] K. Ishfaq, M. Abdullah, and M. A. Mahmood, “A state-of-the-art direct metal laser sintering of Ti6Al4V and AlSi10Mg alloys: Surface roughness, tensile strength, fatigue strength and microstructure,” *Opt. Laser Technol.*, vol. 143, p. 107366, Nov. 2021, doi: 10.1016/j.optlastec.2021.107366.